[RADIOCARBON, VOL 32, NO. 1, 1990, P 37-58]

THE USE OF RADIOCARBON MEASUREMENTS IN ATMOSPHERIC STUDIES[1]

M R MANNING, D C LOWE, W H MELHUISH, R J SPARKS, GAVIN WALLACE, C A M BRENNINKMEIJER and R C McGILL

Institute of Nuclear Sciences, Department of Scientific and Industrial Research
Lower Hutt, New Zealand

ABSTRACT. ^{14}C measured in trace gases in clean air helps to determine the sources of such gases, their long-range transport in the atmosphere, and their exchange with other carbon cycle reservoirs. In order to separate sources, transport and exchange, it is necessary to interpret measurements using models of these processes. We present atmospheric $^{14}CO_2$ measurements made in New Zealand since 1954 and at various Pacific Ocean sites for shorter periods. We analyze these for latitudinal and seasonal variation, the latter being consistent with a seasonally varying exchange rate between the stratosphere and troposphere. The observed seasonal cycle does not agree with that predicted by a zonally averaged global circulation model. We discuss recent accelerator mass spectrometry measurements of atmospheric $^{14}CH_4$ and the problems involved in determining the fossil fuel methane source. Current data imply a fossil carbon contribution of ca 25%, and the major sources of uncertainty in this number are the uncertainty in the nuclear power source of $^{14}CH_4$, and in the measured value for $\delta^{14}C$ in atmospheric methane.

INTRODUCTION

Trace gases in the atmosphere play a crucial role in determining our environment. Greenhouse gases in the troposphere determine the earth's temperature through selective absorption of infra-red radiation. Ozone in the stratosphere filters out ultra-violet radiation that would destroy complex organic molecules essential for life. Because the amounts of these gases are small and the balance of processes maintaining them complex, they are a potentially fragile part of our environment.

Many of the trace gases that must be studied in relation to changes in climate and atmospheric chemistry contain carbon. For these gases, isotopic measurements are directly relevant in determining sources and sinks, because sources will have different isotopic composition and sinks will involve fractionation. The importance of carbon isotope measurements in building global budgets for gases such as CO_2 (Keeling, Mook & Tans 1979; Peng *et al* 1983), CH_4 (Ehhalt 1973) and CO (Stevens *et al* 1972) has been recognized for some time.

The atmospheric concentration of gases with lifetimes of the order of minutes or less is determined by local atmospheric chemistry and the presence or absence of light. For gases with lifetimes of many years, concentrations are relatively homogeneous due to atmospheric mixing. Between these extremes there are atmospheric species with intermediate lifetimes, the concentration of which depends on both atmospheric transport and the distribution of sources and sinks. To understand the varying concentrations of such species, we must combine quantitative information on advection and diffusion in the atmosphere with information on the spatial distribution of sources and sinks. This is a difficult task, but holds the prospect that we may determine a consistent picture of all the processes involved.

Each of the gases CO_2, CH_4 and CO is a candidate for study using a detailed physical and chemical model of the atmosphere. Extensive modeling of the annual cycle of CO_2 concentrations (Trabalka 1985; Heimann & Keeling 1986) has shown that even though this gas has a lifetime in the atmosphere of many years, the latitudinal and seasonal variation of its concentration yields information on long-range atmospheric transport.

CH_4 has a lifetime similar to that of CO_2, but is a complementary tracer of atmospheric transport because the distribution of its sinks is quite different. While the sinks for CO_2 are all at the surface, the dominant sink of CH_4 is through reaction with the OH radical distributed throughout the atmosphere. The OH radical is produced photolytically in the troposphere and its maximum diurnal concentration, and therefore the sink strength for CH_4, varies considerably with latitude, altitude and season (Logan *et al* 1981).

Reaction with the OH radical is also the major sink for CO (Volz, Ehhalt & Derwent 1981), so CO has a sink structure similar to CH_4. As the lifetime of CO ($\approx$4 months) is shorter than the time required to mix throughout the troposphere, this gas does not become

[1] This paper was presented at the 13th International Radiocarbon Conference, June 20–25, 1988 in Dubrovnik, Yugoslavia.

fully dispersed from its sources. In regions where the mean transit time for CO arrival from a source is of the order of its lifetime, we can expect significant variation in concentrations as a result of transient changes in atmospheric transport.

The natural cosmogenic formation of ^{14}C in the stratosphere (Lal & Peters 1962) leads to both ^{14}CO and $^{14}CO_2$. As this ^{14}C production is greatest in the stratosphere, we expect a natural vertical gradient in atmospheric ^{14}C. Human intervention through nuclear weapons testing, which put ^{14}C in the stratosphere, and release of fossil carbon from the surface has enhanced this natural gradient. Relatively rapid mixing in the troposphere can be expected to dissipate this gradient at lower altitudes, but across the tropopause and in the stratosphere it will persist.

Thus, ^{14}C is a useful tracer of transport in the atmosphere, and particularly of vertical transport. The longer-lived species such as $^{14}CO_2$ and $^{14}CH_4$ provide information on the longer time scales associated with stratosphere to troposphere and interhemispheric exchange, whereas ^{14}CO can provide information on the shorter time-scale movements associated with transport within a hemisphere.

We show here that the seasonal component of a 32-yr atmospheric $^{14}CO_2$ record can be used to infer stratospheric residence times for CO_2. Our data are compared with a two-dimensional model of atmospheric transport and discrepancies are shown which imply either deficiencies in present modeling of vertical transport, or the presence of complex sources and sinks of ^{14}C or both. We also show how measurements of $^{14}CH_4$ can identify the relative strengths of fossil and modern sources of methane, and can set limits on the production of this species from nuclear power plants.

MEASUREMENTS OF ATMOSPHERIC $^{14}CO_2$ IN THE SOUTH PACIFIC

Measurements of ^{14}C in atmospheric CO_2 at Wellington, New Zealand and at other South Pacific sites ranging from the Antarctic to the Equator, were initiated by T A Rafter and G J Fergusson in the early 1950s. Early results and procedures are reported elsewhere (Rafter 1955; Rafter & Fergusson 1959; Rafter & O'Brien 1970). Our data report the results of this program up to May 1987.

The sampling procedures used to obtain nearly all the data are described by Rafter and Fergusson (1959). Trays containing ca 2L of 5 normal NaOH carbonate-free solution are exposed for intervals of 1–2 weeks, and the atmospheric CO_2 absorbed during that time is recovered by acid evolution. Considerable fractionation occurs during absorption into the NaOH solution, and the standard fractionation correction (Stuiver & Polach 1977) is used to determine a $\Delta^{14}C$ value corrected to $\delta^{13}C = -25‰$.

A few early measurements were made by bubbling air through columns of NaOH for several hours. These samples can be readily identified in the data as their $\delta^{13}C$ value is much higher (*ie,* closer to the ambient air value). Also, some samples reported here were taken using BaOH solution or with extended tray exposure times. These variations in procedures do not appear to affect the results.

Table 1 lists the Wellington data for the period, Dec 1954–May 1987, and data for shorter periods at six other sites. Dates refer to the mid-point of the sampling interval, and an asterisk denotes a sample for which contamination is known or suspected. Figures 1A, B show the data after discarding these suspect cases.

Low latitudinal gradients are to be expected in the South Pacific, as the sources of $^{14}CO_2$ are far from the sampling sites and CO_2 has a mean lifetime in the atmosphere which is long compared to the time required for tropospheric mixing. This is borne out by our data which show only small variations between sites. Quantifying these differences is made difficult by the noise level, which appears to exceed the error due to counting statistics, and by the sparsity of data from different sites for common times.

Table 2 summarizes the station differences relative to the Wellington station, using months where data are common to both. This suggests that ^{14}C levels in atmospheric CO_2 were slightly higher in the Equatorial Pacific than at mid-southern latitudes, and were

https://doi.org/10.1017/S0033822200039941 Published online by Cambridge University Press

TABLE 1
Radiocarbon measurements of South Pacific air

Date	$\delta^{13}C$ ‰	$\Delta^{14}C$ ‰	Lab number
Tarawa, Kiribati, 1.5° N, 173.0° E			
660805	-21.6	645.7±3.6	NZ2448
661004	-20.9	636.6±3.8	NZ2449
661205	-21.2	649.3±3.8	NZ2452
670205	-21.5	611.6±3.9	NZ2466
670605	-20.9	612.7±3.8	NZ2482
670805	-19.5	600.2±3.8	NZ2481
670905	-19.3	605.6±3.9	NZ2498
671005	-19.5	597.8±3.8	NZ2485
671205	-19.4	594.8±3.8	NZ2484
680305	-19.3	576.1±3.8	NZ2506
680405	-20.5	574.8±3.8	NZ2507
680505	-20.1	567.2±3.8	NZ2508
680605	-20.2	574.0±3.8	NZ2509
680705	-22.8	594.6±6.0	NZ2723
680805	-21.9	557.5±3.5	NZ2721
680830	-20.7	593.8±6.0	NZ2722
680906	-22.6	542.2±3.9	NZ3474
680927	-21.1	553.4±3.9	NZ3479
681025	-21.0	564.1±5.9	NZ2724
681205	-19.4	554.9±3.8	NZ2557
690105	-20.3	548.8±3.8	NZ2558
690305	-21.5	559.1±3.8	NZ2559
690505	-20.6	545.2±3.8	NZ2563
690705	-18.9	536.7±4.0	NZ2569
690905	-18.7	519.4±3.6	NZ2568
691105	-20.6	529.6±3.9	NZ2579
700105	-22.4	533.0±3.8	NZ2578
700305	-21.5	513.6±3.9	NZ2596
700505	-19.9	510.3±3.9	NZ2597
700706	-21.8	507.4±3.9	NZ2608
700905	-21.5	514.0±3.9	NZ2609
701105	-23.1	507.4±3.9	NZ2626
710105	-23.3	507.6±3.9	NZ2627
710306	-22.8	502.7±3.9	NZ2628
710507	-22.7	486.5±3.9	NZ2630
710704	-21.5	486.3±3.7	NZ2655
710904	-21.2	492.0±3.5	NZ2654
711104	-23.5	506.2±3.9	NZ2656
721006	-21.3	460.5±3.6	NZ4095
721104	-21.9	463.6±3.3	NZ4096
721204	-20.5	455.9±3.6	NZ4097
730104	-22.8	442.8±3.3	NZ4098
730205	-22.9	444.8±3.7	NZ2685
730405	-22.7	438.1±3.3	NZ2686
730504	-22.3	452.7±3.7	NZ2687
740804	-21.3	401.8±3.3	NZ4080
740904	-22.5	405.4±3.7	NZ4081
741109	-21.5	394.2±3.6	NZ4099
741204	-21.8	393.9±3.6	NZ4100
750105	-21.3	391.3±3.5	NZ4101
750204	-18.6	376.4±3.3	NZ4102
750605	-22.4	415.5±3.7	NZ4079
750707	-20.8	401.3±3.3	NZ3829
750826	-22.3	390.6±3.3	NZ4141
750904	-23.2	358.9±3.2	NZ4142
751014	-22.8	363.4±3.3	NZ4299
751104	-23.1	366.6±3.3	NZ4300
751204	-22.7	360.4±3.3	NZ5646
760104	-22.6	371.7±3.3	NZ5647
760204	-22.3	354.9±3.3	NZ5648
760304	-22.2	353.4±3.3	NZ5649
760404	-21.2	357.4±3.3	NZ5650
760504	-21.7	348.6±3.7	NZ5651
760612	-20.6	357.8±5.3	NZ5692
760706	-20.6	353.3±3.3	NZ5693
760813	-21.6	352.0±3.7	NZ5694
770812	-16.9	348.4±3.3	NZ5695
Funafuti, Tuvalu, 8.5° S, 179.2° E			
660805	-21.6	650.8±3.8	NZ2446
661005	-21.8	638.5±3.8	NZ2447
661204	-21.9	619.9±3.8	NZ2450
670205	-22.3	636.6±3.8	NZ2465
670505	-20.5	609.9±3.8	NZ2474
670605	-21.1	612.8±3.9	NZ2475
670805	-19.8	596.9±4.5	NZ2476
671005	-20.7	598.9±3.8	NZ2483
671205	-21.8	582.7±4.5	NZ2486
671205	-21.8	586.2±4.5	NZ2489
680305	-20.2	563.6±3.8	NZ2510
680405	-21.0	596.6±3.9	NZ2511
680505	-21.7	561.1±3.8	NZ2512
680602	-19.5	551.4±3.8	NZ2513
680804	-20.7	549.8±3.9	NZ2525
680830	-22.3	556.4±3.9	NZ2526
680906	-18.3	544.0±4.0	NZ2527
680927	-21.1	570.2±5.1	NZ2725
681205	-21.0	553.7±3.8	NZ2536
690105	-18.7	552.6±3.8	NZ2537
690305	-20.7	552.8±3.8	NZ2554
690505	-21.4	535.9±3.9	NZ2561
690705	-20.8	529.1±3.9	NZ2565
690905	-21.2	518.6±3.9	NZ2574
691105	-21.1	517.4±3.9	NZ2575
700105	-21.1	513.5±3.9	NZ2577
700304	-20.6	527.0±3.9	NZ2580
700505	-21.2	523.5±3.9	NZ2594
700705	-21.1	504.5±3.9	NZ2595
701005	-22.3	516.8±3.9	NZ2615
701205	-21.9	517.1±3.9	NZ2616

https://doi.org/10.1017/S0033822200039941 Published online by Cambridge University Press

TABLE 1 (continued)

Date	$\delta^{13}C$ ‰	$\Delta^{14}C$ ‰	Lab number
710205	-22.2	502.6±3.9	NZ2632
710305	-24.2	504.3±3.5	NZ2633
710505	-22.4	512.8±4.0	NZ2634
710705	-22.7	498.7±3.6	NZ2637
710905	-23.0	496.2±3.9	NZ2648
711105	-22.5	487.4±3.5	NZ2649
720106	-22.2	490.0±3.6	NZ2674
720305	-20.8	487.9±3.6	NZ2083
Suva, Fiji, 18.1°S, 178.4°E			
580402	-9.0	74.5±3.8	NZ2000
580407	-25.0	68.4±3.8	NZ2001
580510	-9.0	71.4±3.3	NZ2002
580510	-25.0	69.0±4.7	NZ2003
581104	-25.0	117.1±4.6	NZ2005
590228	-23.6	124.1±4.6	NZ2007
590703	-24.5	151.3±4.1	NZ2004
590922	-22.3	180.4±4.5	NZ2006
600122	-22.1	189.8±4.5	NZ2009
600414	-21.1	185.1±4.5	NZ2008
600902	-22.7	197.0±4.5	NZ2010
600929	-24.6	202.3±4.5	NZ2012
610120	-23.7	196.5±4.5	NZ2011
610301	-21.2	196.8±4.2	NZ2034
610414	-22.9	192.9±5.0	R00945
610708	-22.1	196.5±5.0	NZ2013
610818	-23.1	207.2±4.2	NZ2033
610929	-23.7	180.8±5.0	NZ2015
611110	-23.5	183.5±6.8	R00997
611219	-24.7	198.2±4.9	NZ2014
620119	-21.7	214.4±4.2	NZ2032
620301	-23.2	208.3±5.0	NZ2016
620301	-23.2	233.0±9.4	NZ2092
620412	-21.8	223.5±5.3	NZ2021
620412	-21.8	234.4±4.3	NZ2020
620706	-26.5	238.9±5.9	NZ2091
620927	-24.5	259.3±3.9	NZ2019
630117	-19.8	289.0±4.8	NZ2017
630705	-21.7	380.5±4.1	NZ2022
630917	-22.7	417.6±4.1	NZ2038
630927	-26.8	413.5±4.1	NZ2037
631220	-21.6	497.0±3.4	NZ2024
640116	-21.9	490.7±4.0	NZ2025
640409	-21.9	545.6±3.5	NZ2026
640522	-23.2	548.7±3.5	NZ2027
640702	-26.1	580.4±4.0	NZ2028
640925	-22.6	630.1±3.9	NZ2029
641217	-22.7	644.4±3.7	NZ2030
650115	-19.6	654.5±3.8	NZ2045
650408	-20.2	643.0±3.9	NZ2031
650701	-22.9	647.8±3.9	NZ2035
650813	-22.3	640.1±3.8	NZ2047
650924	-22.9	654.6±3.9	NZ2036
651105	-23.9	653.2±3.8	NZ2041
660106	-22.0	666.5±3.8	NZ2039
660204	-23.4	644.9±3.8	NZ2042
660305	-21.8	635.4±3.8	NZ2040
660605	-23.2	649.0±3.6	NZ2044
660705	-23.3	622.5±3.8	NZ2048
660805	-24.3	626.4±3.9	NZ2043
660905	-23.0	625.8±3.8	NZ2049
661205	-21.4	636.3±3.8	NZ2046
670220	-20.7	616.5±3.8	NZ2050
670714	-22.4	593.1±3.8	NZ2051
670804	-22.4	587.2±3.9	NZ2052
671006	-21.9	584.9±3.9	NZ2054
671205	-21.1	567.9±3.7	NZ2053
680205	-20.8	573.6±3.8	NZ2055
680415	-20.3	567.3±3.8	NZ2056
680604	-19.6	553.7±3.9	NZ2057
680805	-21.5	549.3±3.6	NZ2058
680906	-21.9	545.4±3.6	NZ2059
681005	-20.0	549.4±5.0	NZ2093
681105	-21.7	556.5±3.9	NZ2060
681205	-21.4	530.4±3.8	NZ2061
690105	-20.7	542.4±3.9	NZ2062
690307	-20.0	546.9±3.8	NZ2063
690505	-18.6	531.5±3.6	NZ2064
690706	-20.2	533.8±3.6	NZ2065
690905	-22.1	541.9±3.9	NZ2066
691107	-22.4	531.0±3.9	NZ2067
700109	-21.8	521.7±3.9	NZ2068
700306	-22.1	525.8±3.9	NZ2069
700509	-21.6	536.0±3.9	NZ2070
700705	-21.6	514.3±3.9	NZ2071
700905	-22.1	504.5±3.9	NZ2073
701106	-22.3	506.4±3.9	NZ2072
710108	-21.6	512.1±3.9	NZ2074
710305	-20.6	498.6±3.9	NZ2075
710509	-22.0	492.3±3.9	NZ2076
710710	-22.5	486.9±4.0	NZ2077
710905	-23.2	494.6±3.6	NZ2078
711105	-21.5	498.4±3.9	NZ2079
711205	-21.1	491.4±3.6	NZ2087
720106	-21.4	488.6±3.3	NZ2088
720305	-28.8	501.5±3.6	NZ2080
720505	-21.1	474.3±3.6	NZ2081
720704	-24.5	496.5±6.7	NZ2094
720705	-24.6	473.9±3.3	NZ2082
720805	-20.2	473.4±5.1	NZ2096
721005	-24.1	468.8±3.3	NZ2084
730108	-18.4	458.4±4.6	NZ2095

https://doi.org/10.1017/S0033822200039941 Published online by Cambridge University Press

TABLE 1 (continued)

Date	$\delta^{13}C$ ‰	$\Delta^{14}C$ ‰	Lab number
730205	-21.1	451.3±3.7	NZ2085
730406	-20.4	444.6±3.3	NZ2086
730605	-23.0	433.6±3.3	NZ2090
730805	-23.9	456.2±3.7	NZ2089
731005	-23.9	423.1±3.3	NZ4053
731126	-22.5	430.7±7.4	NZ3816
731207	-21.3	456.5±3.3	NZ4054
740106	-20.9	427.3±3.7	NZ4055
740319	-22.4	409.8±3.7	NZ4059
740405	-21.6	415.2±3.7	NZ4060
740505	-21.4	416.1±4.4	NZ3847
740607	-21.4	403.8±3.7	NZ4061
750307	-21.6	392.6±3.3	NZ4103
750404	-21.8	384.1±3.3	NZ4104
750504	-19.7	379.0±3.3	NZ4105
750608	-22.0	389.3±3.7	NZ4106
Melbourne, Australia, 37.8° S, 144.9° E			
581104	-23.6	76.5±4.0	NZ2311
590229	-24.6	103.3±3.8	NZ2312
590703	-25.1	101.5±4.6	NZ2318
590926	-25.2	136.6±4.5	NZ2319
600122	-22.4	161.5±4.5	NZ2330
600415	-21.4	182.1±4.5	NZ2331
600708	-23.0	155.1±4.6	NZ2335
600930	-21.0	173.0±4.5	NZ2337
601112	-23.5	181.7±4.5	NZ2342
610120	-22.5	188.8±4.5	NZ2343
610929	-20.7	183.2±4.0	NZ2357
611219	-19.0	185.2±4.0	NZ2358
620413	-21.3	198.6±4.0	NZ2359
620928	-22.5	221.8±5.2	NZ3580
630118	-18.2	240.9±4.1	NZ2366
630705	-21.0	282.3±3.9	NZ2388
630926	-20.5	348.9±3.8	NZ2385
631219	-19.4	411.5±3.8	NZ2386
640116	-21.6	436.8±3.8	NZ2387
640410	-19.7	486.6±4.0	NZ2397
640702	-20.3	512.0±4.0	NZ2398
640925	-20.2	560.3±3.9	NZ2400
641218	-20.5	574.4±3.9	NZ2399
650115	-20.6	609.3±3.8	NZ2459
650409	-20.1	608.0±3.9	NZ2422
650520	-19.8	589.8±3.8	NZ2460
651001	-20.9	612.5±3.8	NZ2423
651105	-20.9	620.7±3.8	NZ2430
651205	-20.1	516.9±3.9	NZ2461
660107	-20.2	610.2±3.8	NZ2424
660305	-21.1	614.0±3.8	NZ2438
660505	-22.8	614.9±3.8	NZ2437
660605	-20.5	587.3±3.9	NZ2440
660905	-28.0	631.6±3.8	NZ2456
661005	-23.1	614.3±3.8	NZ2455
661205	-20.5	602.8±3.8	NZ2457
670205	-16.1	592.4±3.8	NZ2470
670606	-20.3	501.3±4.5	NZ2473
670705	-19.5	516.3±3.9	NZ2497
670805	-20.8	535.3±3.6	NZ2472
670905	-21.5	575.3±3.9	NZ2496
680205	-20.2	561.1±3.9	NZ2500
680405	-19.4	562.3±3.9	NZ2501
680605	-21.0	529.1±3.9	NZ2517
680704	-22.5	517.8±3.9	NZ3468
680804	-20.3	503.5±3.9	NZ2519
680828	-20.2	533.1±3.9	NZ2518
680905	-25.0	531.7±3.9	NZ2533
680926	-21.7	509.7±3.9	NZ2534
681003	-19.8	515.9±3.9	NZ3495
681031	-22.8	521.8±3.9	NZ3480
681107	-22.3	535.0±3.9	NZ3482
681205	-19.7	512.7±3.9	NZ2532
690105	-19.5	534.8±3.8	NZ2555
690305	-19.3	532.6±3.9	NZ2556
690505	-19.7	496.6±3.9	NZ2562
690705	-20.6	496.3±3.4	NZ2581
690906	-20.6	488.3±3.9	NZ2586
691104	-19.0	507.0±3.9	NZ2588
700105	-18.0	515.8±3.9	NZ2587
700305	-19.4	509.0±3.9	NZ2620
700505	-20.0	486.7±3.9	NZ2621
700701	-20.3	475.6±3.9	NZ2622
700905	-19.7	486.5±3.9	NZ3547
701104	-20.3	480.3±3.5	NZ3548
710105	-19.2	484.6±3.9	NZ2625
710604	-17.9	433.1±3.9	NZ2650
710804	-18.8	463.6±3.5	NZ2651
711004	-19.6	462.3±3.9	NZ2652
711204	-18.4	470.5±3.5	NZ2653
720604	-18.8	398.1±6.7	NZ2733
Wellington, New Zealand, 41.3° S, 174.8° E			
541215	-9.4	-17.7±7.6	NZ2100
550222	-9.4	-10.1±7.7	NZ2099
550414	-9.4	-1.4±7.6	NZ2098
550510	-24.9	-10.3±7.8	NZ2097
550615	-9.4	-4.1±5.9	NZ2102
550907	-8.8	-11.9±4.0	NZ2103
551215	-8.8	0.1±5.4	NZ2104
560219	-8.8	5.6±3.9	NZ2105
560615	-25.0	37.9±4.8	NZ2107
560925	-25.8	10.1±4.8	NZ2108
561021	-9.0	13.6±4.7	NZ2110

TABLE 1 (continued)

Date	$\delta^{13}C$ ‰	$\Delta^{14}C$ ‰	Lab number
561022	-9.2	18.1±4.7	NZ2109
570127	-9.0	18.3±3.7	NZ2111
570127	-10.1	24.9±3.7	NZ2112
570428	-10.6	39.0±4.7	NZ2113
570428	-9.8	41.5±4.7	NZ2114
570522	-24.8	16.6±4.8	NZ2115
570723	-9.4	44.9±3.9	NZ2120
570723	-9.6	43.4±3.9	NZ2118
570827	-24.8	51.4±4.0	NZ2116
571009	-12.5	46.3±5.1	NZ2122
571106	-9.7	51.6±4.7	NZ2124
571126	-8.8	62.0±4.6	NZ2123
580318	-9.4	67.5±4.0	NZ2126
580318	-10.1	76.2±4.0	NZ2125
580704	-25.0	81.1±3.8	NZ2128
580828	-25.0	77.8±3.8	NZ2127
580929	-24.8	93.9±3.5	NZ2129
581009	-24.6	116.9±4.6	NZ2130
581223	-25.0	110.1±3.8	NZ2131
590117	-25.0	121.1±3.8	NZ2132
590302	-25.0	126.0±4.6	NZ2133
590411	-25.1	137.2±3.8	NZ2134
590601	-25.9	132.8±3.8	NZ2136
590713	-25.2	150.1±3.8	NZ2135
590813	-25.0	141.8±4.5	NZ2137
591001	-26.4	164.6±4.5	NZ2138
591119	-24.5	171.4±4.5	NZ2139
591219	-25.0	181.7±4.5	NZ2140
600121	-25.2	181.8±4.5	NZ2141
600414	-23.4	187.9±4.5	NZ2142
600714	-24.0	187.4±4.5	NZ2143
600901	-22.8	193.7±4.5	NZ2145
600929	-22.5	195.9±4.5	NZ2144
601113	-26.4	198.4±4.5	NZ2147
601219	-24.5	193.7±4.5	NZ2146
610120	-25.5	194.9±4.5	NZ2148
610310	-24.9	207.1±5.1	NZ2149
610414	-25.0	201.9±4.5	NZ2150
610526	-26.3	196.7±4.5	NZ2151
610706	-25.1	198.3±9.5	NZ2263
610819	-25.3	197.9±6.3	NZ2262
611003	-24.7	182.8±5.0	NZ2152
611111	-23.8	237.2±9.4	NZ2264
611219	-25.1	227.3±9.4	NZ2265
620119	-24.6	197.4±5.0	NZ2268
620302	-23.4	207.3±7.5	NZ2266
620425	-24.5	214.3±5.1	NZ2267
620525	-24.5	189.4±9.5	NZ2269
620928	-24.5	233.5±4.4	NZ2155
621109	-24.0	250.4±5.9	NZ2270
621220	-28.4	266.6±3.9	NZ2153
630118	-25.9	265.5±3.9	NZ2154
630301	-23.6	269.7±3.9	NZ2156
630301	-23.6	266.4±3.8	NZ2159
630414	-23.5	280.9±3.8	NZ2160
630414	-23.5	284.3±3.9	NZ2157
630526	-24.2	313.2±4.1	NZ2163
630706	-24.7	331.1±4.1	NZ2161
630817	-24.7	355.6±4.3	NZ2162
630929	-23.7	405.2±3.8	NZ2164
631110	-24.7	374.8±4.1	NZ2165
631220	-24.7	429.5±3.8	NZ2166
640117	-23.1	445.7±3.8	NZ2167
640301	-22.8	472.5±4.0	NZ2168
640411	-23.7	500.3±4.0	NZ2169
640523	-25.9	498.3±3.9	NZ2170
640703	-24.7	542.4±3.7	NZ2171
640815	-24.6	567.4±4.0	NZ2173
641003	-25.4	507.0±3.9	NZ2172
641106	-24.7	621.9±3.9	NZ2174
641217	-19.9	615.7±3.9	NZ2175
650115	-22.0	689.4±7.5	NZ2271
650227	-23.6	633.6±3.9	NZ2176
650408	-23.9	634.1±3.9	NZ2178
650521	-21.4	615.2±3.8	NZ2177
650702	-25.7	694.5±3.9	NZ2180
650813	-23.9	614.1±3.9	NZ2179
650924	-25.2	634.2±4.0	NZ2181
651106	-18.1	625.7±4.0	NZ2182
651224	-24.9	634.4±3.9	NZ2183
660204	-24.6	647.3±3.9	NZ2184
660308	-26.4	646.5±3.9	NZ2185
660402	-23.9	631.8±3.6	NZ2186
660520	-26.1	622.1±3.8	NZ2189
660610	-25.0	612.4±4.2	NZ2188
660706	-23.2	612.2±4.4	NZ2187
660819	-24.8	590.8±3.9	NZ2190
660909	-26.8	625.2±3.8	NZ2191
661007	-23.8	614.8±3.9	NZ2192
661105	-25.1	614.9±4.2	NZ2193
661211	-24.8	627.8±3.9	NZ2194
670109	-24.6	616.4±3.9	NZ2195
670224	-23.0	602.9±4.4	NZ2196
670408	-23.4	609.0±3.8	NZ2197
670506	-23.7	596.5±3.8	NZ2198
670610	-23.7	580.0±6.3	NZ2272
670610	-23.7	595.9±5.4	NZ2273
670719	-24.4	571.3±3.8	NZ2199
671006	-23.1	575.1±3.8	NZ2200
671110	-25.7	586.0±5.2	NZ2274
671209	-24.4	579.6±3.9	NZ2201
680113	-23.9	583.0±3.9	NZ2202

TABLE 1 (continued)

Date	$\delta^{13}C$ ‰	$\Delta^{14}C$ ‰	Lab number
680211	-24.5	582.5±3.9	NZ2203
680311	-22.5	572.8±3.6	NZ2204
680406	-23.9	547.6±3.7	NZ2205
680531	-24.8	560.5±3.9	NZ2206
680607	-24.6	561.7±3.9	NZ2207
680705	-26.3	550.4±3.9	NZ2208
680809	-24.7	538.1±3.9	NZ2209
680830	-23.8	535.5±3.8	NZ2210
680906	-23.7	531.5±3.9	NZ2211
681004	-24.6	532.8±3.9	NZ2212
681018	-24.7	537.6±3.9	NZ2213
681102	-25.3	541.9±3.9	NZ3470
681108	-26.9	541.2±3.9	NZ2214
681206	-23.8	539.6±3.9	NZ2215
690110	-24.3	539.1±3.9	NZ2217
690207	-23.1	537.7±3.8	NZ2216
690308	-23.3	550.4±3.8	NZ2218
690413	-23.4	545.4±3.8	NZ2222
690502	-23.1	530.4±4.0	NZ2220
690509	-22.8	539.6±3.9	NZ2221
690607	-23.4	525.2±4.2	NZ2223
690711	-23.2	526.3±3.9	NZ2219
690809	-23.0	522.8±3.9	NZ2224
690905	-23.5	544.9±3.8	NZ2225
691010	-25.2	531.2±3.9	NZ2226
691103	-23.2	523.0±3.9	NZ2227
691205	-22.5	510.2±3.9	NZ2228
700109	-22.5	510.2±3.9	NZ2229
700306	-22.5	535.3±3.9	NZ2230
700410	-22.1	520.4±3.9	NZ2232
700509	-22.4	513.5±3.9	NZ2231
700606	-23.3	516.2±3.9	NZ2233
700710	-23.8	505.9±3.9	NZ2234
700807	-23.6	497.4±3.5	NZ2235
700911	-24.5	508.0±3.9	NZ2236
701010	-24.3	498.6±3.9	NZ2237
701106	-23.3	497.6±4.0	NZ2238
701223	-22.7	495.6±3.9	NZ2239
710110	-22.3	500.6±3.9	NZ2240
710205	-23.8	494.7±3.7	NZ2241
710305	-24.6	508.3±3.9	NZ2242
710409	-24.8	501.0±3.9	NZ2243
710507	-24.9	499.7±3.9	NZ2244
710611	-24.6	499.0±3.9	NZ2245
710709	-25.9	494.2±4.1	NZ2246
710808	-23.5	483.3±4.0	NZ2248
710910	-24.5	478.8±4.5	NZ2247
711010	-24.0	492.5±3.9	NZ2249
711203	-24.8	479.3±3.9	NZ2251
720109	-23.9	484.5±3.6	NZ2252
720206	-24.7	491.6±4.0	NZ2253
720317	-22.5	474.8±7.4	NZ2282
720331	-23.8	482.4±3.6	NZ2250
720420	-22.6	468.1±3.6	NZ2254
720504	-23.0	469.5±5.1	NZ2286
720610	-24.4	470.1±5.1	NZ2287
720707	-24.0	465.9±5.1	NZ2288
720901	-24.7	450.3±5.1	NZ2289
721007	-24.4	449.9±6.7	NZ2283
721208	-24.9	447.3±4.7	NZ2285
730210	-24.3	453.9±5.1	NZ2291
730309	-23.6	442.8±3.3	NZ2255
730706	-24.7	435.0±3.7	NZ2256
730811	-24.5	427.1±3.3	NZ2257
730907	-24.4	415.9±3.7	NZ2258
731006	-24.1	426.0±3.3	NZ2259
731109	-23.4	434.3±3.7	NZ2260
731207	-23.3	417.2±3.2	NZ2261
740111	-23.2	412.8±3.5	NZ3565
740201	-23.0	405.1±3.3	NZ3566
740308	-22.2	418.5±3.3	NZ3567
740404	-23.0	417.2±3.3	NZ3568
740510	-23.3	386.8±3.3	NZ3572
740607	-23.3	359.7±3.3	NZ4052
740706	-23.3	394.5±3.3	NZ4057
740807	-24.8	392.3±3.7	NZ4058
740906	-23.4	405.0±3.3	NZ4062
741005	-23.2	398.7±4.7	NZ3848
741108	-22.8	401.7±3.3	NZ4065
741208	-23.4	393.7±3.3	NZ4074
750110	-22.2	396.3±3.3	NZ4076
750207	-23.4	399.0±3.7	NZ4078
750307	-23.3	400.6±3.3	NZ4083
750405	-23.4	397.7±3.3	NZ4088
750510	-23.2	389.1±3.7	NZ4090
750620	-23.9	384.5±3.3	NZ4092
750709	-23.1	377.3±3.3	NZ4094
750810	-24.9	378.1±3.7	NZ4108
750912	-26.2	367.5±3.7	NZ4110
751003	-23.6	354.0±8.8	NZ4121
751010	-22.4	365.3±3.3	NZ4119
751115	-23.0	363.8±3.7	NZ4122
751205	-23.6	370.8±3.7	NZ4124
760113	-23.8	373.4±3.7	NZ4126
760206	-24.3	368.1±3.3	NZ4135
760306	-23.7	366.7±3.1	NZ4137
760410	-23.0	346.1±3.3	NZ4145
760510	-22.9	359.6±3.3	NZ4140
760606	-25.0	360.9±3.4	NZ4144
760704	-22.2	365.0±5.0	NZ4302
760815	-23.9	343.3±3.7	NZ5659
761011	-22.9	344.2±5.1	NZ5673

TABLE 1 (continued)

Date	$\delta^{13}C$ ‰	$\Delta^{14}C$ ‰	Lab number
761104	-25.3	346.5±3.3	NZ5675
761210	-23.6	329.6±3.7	NZ5678
770103	-24.5	332.9±3.7	NZ5679
770211	-24.3	347.0±5.3	NZ5688
770311	-24.7	335.4±4.5	NZ5690
770506	-24.8	332.9±3.3	NZ5697
770612	-24.1	335.6±4.7	NZ5699
770715	-22.4	331.5±3.7	NZ5900
770813	-24.1	323.6±3.3	NZ5702
770909	-24.8	317.6±3.3	NZ5707
771001	-28.1	335.1±3.4	NZ5730
771007	-24.2	322.0±3.7	NZ5731
771111	-23.4	325.0±3.7	NZ5732
780502	-24.6	314.6±3.7	NZ5866
780611	-25.8	310.4±3.7	NZ5867
780630	-25.9	314.8±3.7	NZ5868
780804	-25.2	308.8±3.2	NZ5869
780908	-18.0	309.0±5.1	NZ5870
781007	-25.5	321.3±8.9	NZ5871
781110	-25.4	308.1±3.3	NZ5872
790112	-24.9	310.2±3.3	NZ5910
790317	-24.7	302.8±3.3	NZ5911
790407	-25.3	304.2±3.7	NZ5912
790509	-24.9	296.2±3.2	NZ5913
790603	-24.5	292.3±3.3	NZ5914
790710	-24.9	298.6±3.8	NZ5915
790812	-25.4	284.0±3.8	NZ5916
791005	-25.3	282.9±3.7	NZ5956
791103	-25.2	303.5±3.8	NZ5957
791209	-24.3	276.4±3.3	NZ5958
800212	-25.3	282.3±3.3	NZ5959
800308	-25.1	289.0±3.8	NZ5960
800404	-24.8	277.6±3.3	NZ5961
800508	-23.7	279.4±3.3	NZ5969
800616	-23.5	* 239.1±7.9	NZ5971
800706	-25.4	281.5±3.7	NZ6008
800801	-25.0	274.3±3.7	NZ6009
800905	-24.8	278.1±3.3	NZ6010
801009	-25.5	282.7±3.7	NZ6011
801111	-25.6	272.9±3.2	NZ6012
801204	-25.4	268.6±3.4	NZ6013
810110	-24.7	266.0±3.7	NZ6014
810206	-25.4	260.9±3.7	NZ6015
810312	-24.0	264.1±4.7	NZ6016
810410	-25.2	270.9±3.3	NZ6017
810507	-24.5	* 352.2±3.3	NZ6421
810606	-26.2	263.3±3.7	NZ6062
810809	-26.1	259.5±3.3	NZ6063
810904	-25.1	258.0±5.1	NZ6064
811002	-26.0	256.8±3.3	NZ6065
811101	-25.4	254.7±3.7	NZ6066
811203	-25.4	254.8±3.2	NZ6067
820402	-25.4	* 385.6±3.7	NZ6432
820509	-23.5	245.2±3.2	NZ6449
820605	-25.0	248.5±3.2	NZ6450
820708	-23.3	249.2±3.8	NZ6451
820902	-25.8	241.3±3.2	NZ6459
821206	-25.2	235.5±3.4	NZ6523
830117	-24.1	233.6±3.7	NZ6527
830207	-24.9	227.4±3.7	NZ6528
830306	-25.8	233.9±3.3	NZ6529
830519	-2.2	* 398.4±15.5	NZ6623
830607	-25.2	235.6±3.7	NZ6530
830819	-25.0	235.0±3.7	NZ6538
831015	-24.9	221.2±3.7	NZ6539
831029	-7.3	* 290.0±9.6	NZ6624
840115	-25.0	217.5±3.3	NZ6540
840205	-24.2	230.3±3.8	NZ6549
840508	-25.3	214.0±3.8	NZ6816
840610	-25.9	* 244.8±4.5	NZ6815
840709	-25.3	214.5±3.8	NZ6817
840803	-26.4	238.0±4.4	NZ6807
840910	-25.4	208.1±3.5	NZ6820
841111	-25.4	206.9±2.7	NZ6821
841202	-26.4	216.8±3.3	NZ6831
850202	-26.5	206.9±3.3	NZ6847
850324	-25.4	209.8±3.8	NZ6858
850706	-27.2	218.0±8.0	NZ7257
850809	-25.7	213.0±6.0	NZ7277
850909	-25.8	204.0±6.0	NZ7272
851102	-26.0	203.4±4.2	NZ7408
851202	-26.6	205.1±4.2	NZ7409
860110	-23.7	204.0±4.0	NZ7264
860214	-26.0	207.0±5.0	NZ7286
860331	-26.0	199.0±5.0	NZ7382
860502	-23.5	184.0±7.0	NZ7417
860712	-25.8	194.5±4.2	NZ7410
860810	-26.5	188.3±3.7	NZ7412
860907	-26.1	200.8±3.7	NZ7413
861005	-26.0	194.0±4.0	NZ7430
861108	-25.5	191.0±4.0	NZ7431
861207	-25.6	189.0±4.0	NZ7432
870103	-25.5	185.0±4.0	NZ7454
870405	-25.6	189.0±5.6	NZ7395
870510	-25.5	190.0±4.2	NZ7455
870609	-25.8	176.2±4.6	NZ7456
Campbell Is, New Zealand, 52.5° S, 169.2° E			
700105	-25.2	501.6±3.9	NZ2600
700305	-23.7	511.0±3.9	NZ2601
700504	-24.4	512.5±3.9	NZ2604
700710	-25.2	496.7±3.9	NZ2607

https://doi.org/10.1017/S0033822200039941 Published online by Cambridge University Press

TABLE 1 (continued)

Date	$\delta^{13}C$ ‰	$\Delta^{14}C$ ‰	Lab number
700904	-25.6	486.7±3.6	NZ2662
701104	-24.9	482.6±3.9	NZ2663
710106	-24.3	494.0±3.9	NZ2664
710307	-23.3	504.6±3.9	NZ2665
710404	-18.3	506.1±3.9	NZ2666
710704	-25.2	489.9±3.7	NZ2667
710904	-26.1	483.7±5.2	NZ2742
730105	-26.2	453.9±5.2	NZ2743
731008	-22.7	409.8±3.7	NZ2690
731108	-25.2	406.4±3.3	NZ2691
731206	-26.1	403.3±3.3	NZ2692
740115	-24.8	404.8±3.3	NZ2693
740304	-25.4	411.5±3.7	NZ4066
740404	-25.1	403.2±3.3	NZ4067
740506	-26.1	412.2±3.7	NZ4068
740607	-25.9	408.4±3.3	NZ4069
740706	-25.9	401.1±3.7	NZ4070
740804	-24.8	402.8±3.7	NZ4071
740904	-25.4	397.2±3.7	NZ4072
740908	-26.6	400.4±3.7	NZ4084
741004	-25.2	420.2±3.2	NZ5644
741104	-24.1	402.2±3.3	NZ4086
741208	-22.9	393.5±7.4	NZ3835
750112	-23.3	393.7±5.1	NZ4127
750204	-24.4	374.5±4.6	NZ4128
750313	-24.3	389.3±3.7	NZ4111
750417	-25.7	395.3±5.1	NZ4112
750506	-25.2	385.1±5.5	NZ4113
750608	-25.4	400.4±5.8	NZ4114
750707	-26.1	368.4±3.3	NZ4115
750813	-25.1	359.7±3.7	NZ4116
750908	-22.7	359.9±3.2	NZ4117
751008	-26.8	373.2±3.3	NZ4129
751105	-25.1	368.9±3.7	NZ4130
751204	-25.9	364.0±3.3	NZ4131
760104	-24.7	370.4±3.3	NZ4132
760204	-25.4	363.8±3.7	NZ4133
760304	-25.3	353.6±3.7	NZ5666
760406	-25.3	362.1±3.3	NZ5667
760504	-24.3	352.5±3.2	NZ5668
760604	-25.5	350.2±3.5	NZ5669
760704	-24.8	351.4±3.3	NZ5670
760803	-25.2	344.0±3.3	NZ5671
760904	-25.3	343.0±3.2	NZ5681
761004	-24.9	330.4±3.2	NZ5682
761104	-25.3	333.3±3.7	NZ5683
761204	-25.2	342.0±3.3	NZ5684
770104	-24.3	337.7±3.3	NZ5685
770204	-23.5	334.3±3.7	NZ5686

Date	$\delta^{13}C$ ‰	$\Delta^{14}C$ ‰	Lab number
Scott Base, Antarctica, 77.9° S, 166.7° E			
611105	-26.1	195.7±6.4	NZ2695
611230	-25.6	196.7±9.6	NZ3577
620207	-27.7	180.3±9.9	NZ3575
620228	-27.4	203.2±6.3	NZ3573
621201	-32.3	251.5±3.9	NZ2373
630107	-29.1	255.8±4.1	NZ2374
660102	-26.1	622.0±3.8	NZ2426
660124	-23.1	635.2±3.9	NZ2417
660205	-23.8	622.5±3.8	NZ2427
660217	-14.9	633.3±3.6	NZ2418
671202	-23.4	573.8±3.9	NZ2493
671229	-24.6	577.6±3.9	NZ2494
680129	-21.3	539.3±5.2	NZ2715
680212	-17.6	573.6±3.9	NZ2495
681121	-23.2	539.1±3.8	NZ2547
681216	-25.0	542.3±3.9	NZ2548
690110	-24.6	545.1±3.8	NZ2549
690208	-26.3	542.4±3.9	NZ2550
691106	-19.4	556.6±8.8	NZ2729
691227	-19.2	476.1±7.3	NZ2730
700116	-16.4	492.4±7.3	NZ2731
710408	-22.9	496.2±3.5	NZ2658
710420	-24.5	497.3±3.9	NZ2657
710714	-24.5	479.5±3.6	NZ2659
711112	-27.8	477.7±4.0	NZ2661
711218	-26.5	477.5±4.0	NZ2660
730215	-20.5	447.3±3.7	NZ2682
730412	-23.6	433.7±5.2	NZ2747
730914	-25.0	432.4±4.5	NZ2750
731019	-20.3	438.0±6.8	NZ2738
740423	-22.6	406.7±5.2	NZ3849
740513	-18.2	400.1±6.9	NZ3825
740816	-19.0	340.8±8.7	NZ3826
751008	-16.6	403.8±5.2	NZ3850
751123	-26.1	361.7±3.3	NZ5660
751230	-25.6	361.6±3.3	NZ5661
760130	-25.5	368.9±3.3	NZ5662
760316	-22.4	374.0±5.1	NZ5663

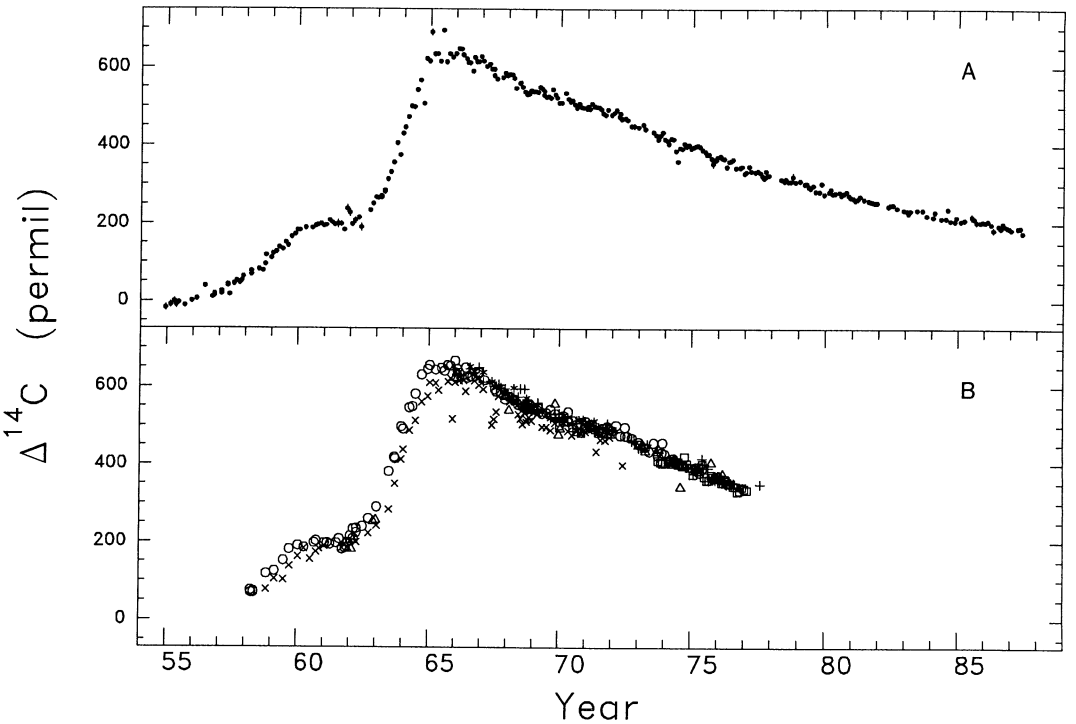

Fig 1. $\Delta^{14}C$ values measured in atmospheric CO_2 at (A) Wellington, New Zealand and (B) other sites in the South Pacific, 1954–1987. Symbols used in (B) are: + Tarawa Is, 1.5°N; ∗ Funafuti, 8.5°S; O Suva, 18.1°S; × Melbourne, 37.8°S; □ Campbell Is, 52.5°S; and △ Scott Base, 77.9°S.

slightly lower at higher latitudes during 1966–1976. The data from Melbourne are ca 25‰ lower than the Wellington data, and as pointed out by Rafter and O'Brien (1970), this is likely to be due to a local effect of fossil-fuel carbon at the monitoring site which was a rooftop in the center of Melbourne city.

The ^{14}C record for the South Pacific in Figures 1 A, B clearly shows a peak in 1965 occurring a little over one year later than that observed in the Northern Hemisphere (Nydal & Lovseth 1983; Levin *et al* 1985). Although Northern Hemisphere surface measurements of $^{14}CO_2$ were higher than those reported here in the mid-1960s, this difference had disappeared by 1968. From 1980 onwards, the Southern Hemisphere $\Delta^{14}C$ values appear slightly higher than those measured in Europe. This is consistent with a regional "Suess" effect influencing the European data. The continuing fall of excess $^{14}CO_2$ has a 1/e time of ca 17 yr.

TABLE 2

$\Delta^{14}C$ for South Pacific sites relative to Wellington statistics of differences in data for the same month

Site	No of common months	Median difference	Mean difference	Standard deviation about mean
Tarawa, 1.5°N	58	8.7	7.3	16.2
Funafuti, 8.5°S	34	8.6	10.2	17.0
Suva, 18.1°S	86	8.7	8.7	20.3
Melbourne, 37.8°S	60	-22.3	-27.0	23.4
Campbell Is, 52.5°S	50	-6.4	-3.5	13.9
Scott Base, 77.9°S	29	-4.5	-6.6	21.1

https://doi.org/10.1017/S0033822200039941 Published online by Cambridge University Press

The seasonal structure in the region of the peak Southern Hemisphere values is much less pronounced than for Northern Hemisphere data. This, together with the later arrival of the peak in the Southern Hemisphere, is consistent with the fact that most of the release of ^{14}C from nuclear weapons testing occurred in the Northern Hemisphere. Further, it is well established (Telegadas 1971) that most of the ^{14}C inventory produced by nuclear tests was located in the stratosphere by the mid-1960s. Figure 2 shows this stratification of the ^{14}C inventory between the stratosphere and troposphere by comparing surface data (Levin *et al* 1985; this work), with tropospheric and stratospheric data (Telegadas 1971).

ANALYSIS OF $^{14}CO_2$ DATA

We average all the data (usually just one value) available for Wellington in each month in order to obtain a time series spanning 391 months with 104 missing values. The missing data are fairly evenly distributed through the record and so are unlikely to bias the following analysis.

In order to extract a seasonal component, we must determine a smooth trend in the data about which the seasonal variation occurs. There are many procedures for doing this (eg, Cleveland Freeny & Graedel 1983; Enting 1987). The methods used here are based on "loess" smoothing (Cleveland 1979) and the "STL" procedure for seasonal and trend decomposition (Cleveland & McRae 1989).

Loess smoothing determines a smoothed value at each point in the series from a window of a fixed number of nearest neighbors. The smoothed value is determined by fitting a straight line to the data window using weights that decrease with distance from the subject point. Both loess smoothing and the STL procedure are robust with respect to outliers, *ie*,

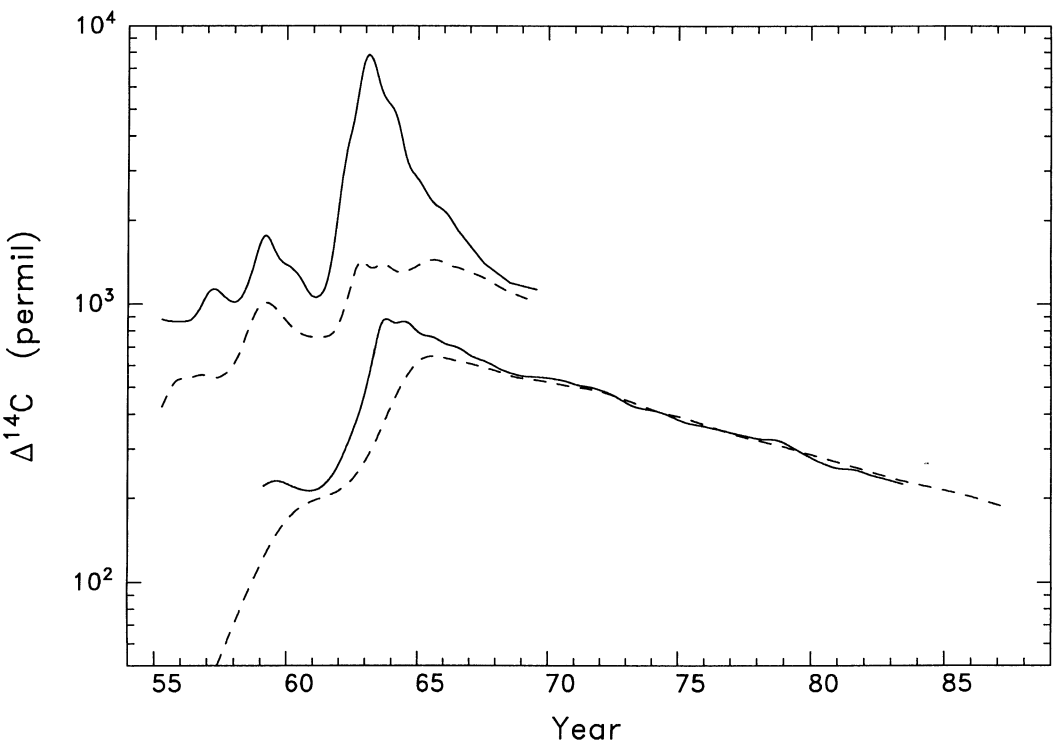

Fig 2. $\Delta^{14}C$ values in the stratosphere and at the earth's surface shown as smooth spline curves fitted to available data; the upper two curves are for the stratosphere and the lower two for the surface; ___ denotes Northern Hemisphere and – – – – Southern Hemisphere. Based on stratospheric data from Telegadas (1971), Northern Hemisphere surface data from Levin *et al* (1985) and Southern Hemisphere surface data from this work.

https://doi.org/10.1017/S0033822200039941 Published online by Cambridge University Press

outlier points are identified by an initial calculation, their weights are reduced and the calculation repeated. The STL procedure determines the seasonal and trend components simultaneously with a consistent philosophy of the structure of each. The trend component is determined by loess smoothing of the data minus the seasonal component, the latter being determined for each calendar month by loess smoothing of the data minus the trend component. STL allows arbitrary variation of the seasonal component from month to month within the year (in contrast to band pass filtering methods) but ensures small variation in the seasonal cycle from year to year.

There are inherent difficulties in separating seasonal and trend components for both the rapid rise in $\Delta^{14}C$ values during the early 1960s and the following decay. Further, the relative distribution of ^{14}C throughout the atmosphere may have been significantly altered by the very large tesss of the early 1960s. Thus, in order to determine a consistent and slowly varying seasonal component, we have limited the analysis to 1966 onwards.

The STL procedure does not allow for missing data, so missing values have been interpolated by fitting a Reinsch (1967) spline to the data, and adjusting the tension of the spline so that the number of sign changes in residuals agrees with that expected for a random sequence. We have tried alternative procedures for interpolating missing data which do not significantly affect the results. Figures 3A, B, C, show the trend, seasonal and remainder components. The seasonal component shows a cycle of decreasing amplitude with some evidence of a phase change in the latter part of the record.

Up to 1980, the cycle has a maximum in March and a minimum in August; a negative anomaly occurs in December. The amplitude of the cycle decreases steadily from a peak-to-peak range of 20‰ in 1966 to 3‰ in 1980. From 1966–1975, while the shape of the cycle is roughly constant, the amplitude decays exponentially with a 1/e time of 12 yr. From 1980 onwards, a different cycle emerges with an amplitude of ca 5‰, a maximum in July– August

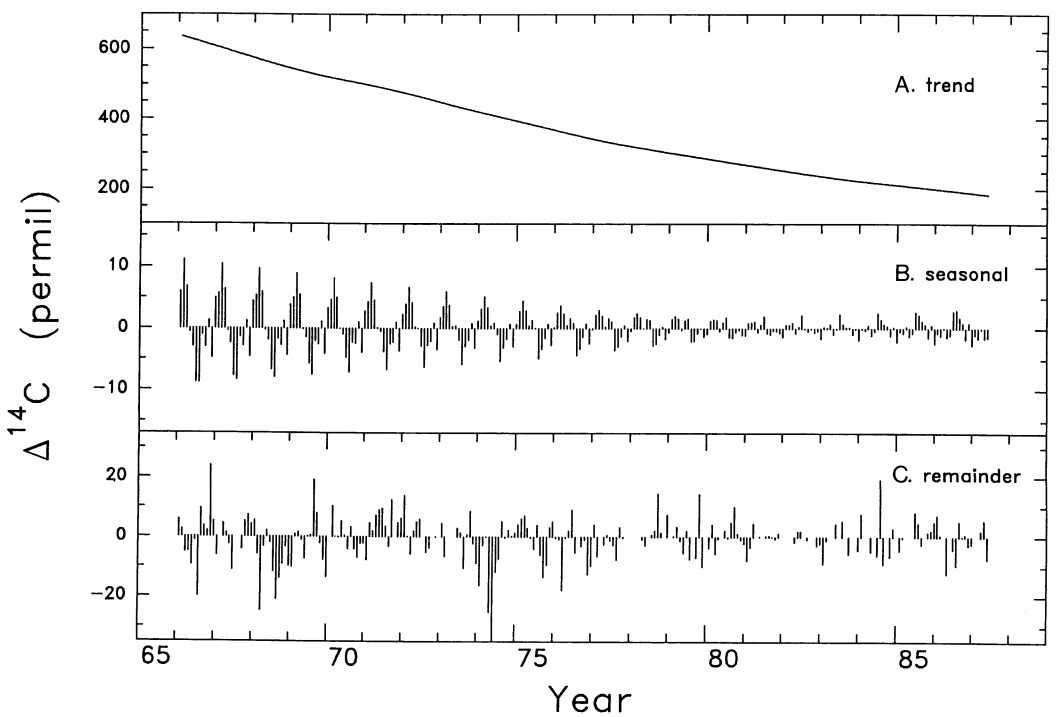

Fig 3. The (A) smooth trend, (B) seasonal and (C) remainder components of the Wellington $\Delta^{14}C$ data record determined by the STL procedure as discussed in the text.

https://doi.org/10.1017/S0033822200039941 Published online by Cambridge University Press

and minimum in January. If present, this would have been masked in the earlier part of the record by the larger decaying cycle.

A direct indication of the change in the seasonal cycle can be seen by plotting the differences of the original data from a smooth trend, against a calendar month. Figures 4A, B show such "month-plots" of differences from the smooth trend, in the periods 1966–1977 and 1981–1987. Horizontal bars show the mid-mean (mean of values between the upper and lower quartiles) of all data for a given month. Individual data values are shown by a spike from the mid-mean for the corresponding month. The contrast in the annual cycle for these two periods confirms that the change in the seasonal cycle is not an artifact of the interpolation or outlier rejection techniques used with the STL procedure.

Finally, we note that the seasonal cycles at the other South Pacific sites are not well determined by our data, and for some months the differences between sites are large compared with errors due to counting statistics. These appear often enough to suggest that regional variations in $^{14}CO_2$ may be as large as 20‰.

INTERPRETATION OF $^{14}CO_2$ SEASONAL AND TREND VARIATION

The overall decline in atmospheric $^{14}CO_2$ has been studied extensively in many analyses of the global carbon cycle (Oeschger *et al* 1975; Enting & Pearman 1983). This decline is predominantly determined by the rate of exchange of carbon between the atmosphere and the ocean, and is one of the best determinants of that exchange rate.

Although the seasonal cycle in atmospheric $^{14}CO_2$ has not been well researched, seasonal cycles in other "bomb"-produced radionuclides, particularly ^{90}Sr and ^{3}H, are influenced by seasonal changes in transport of stratospheric air into the troposphere. The transport of gaseous tracers such as $^{14}CO_2$ is by advection and diffusion, whereas for other radionuclides particulate deposition and rainout phenomena are dominant (Sarmiento & Gwinn 1986; Schell, Sauzay & Payne 1974). Thus, differences between the seasonal cycle of $^{14}CO_2$ and other fallout species are expected.

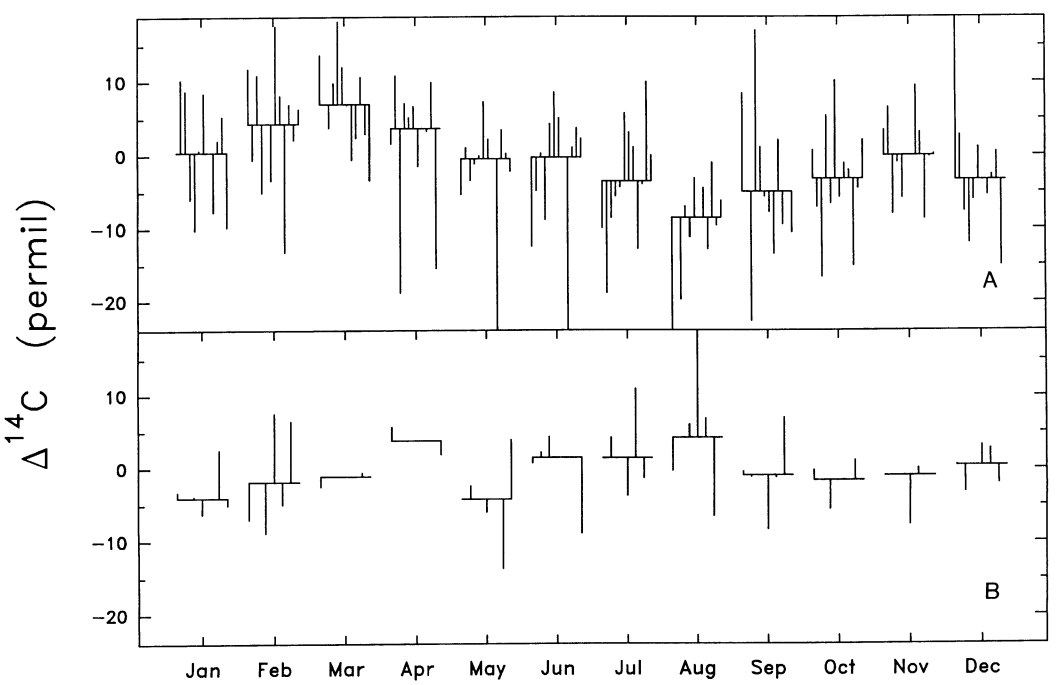

Fig 4. Seasonal cycles of differences between $\Delta^{14}C$ data and their smooth trend. Data are grouped by calendar month and shown as spikes from the mid-mean, (A) for period 1966–1977 and (B) for period 1981–1987.

https://doi.org/10.1017/S0033822200039941 Published online by Cambridge University Press

Factors other than transport from the stratosphere also contribute to seasonal variation in $^{14}CO_2$. Levin (1985) reports variations at a European site due to seasonal changes in the release of fossil-fuel CO_2, and at an Antarctic site due to seasonal changes in ocean-atmosphere exchange.

The seasonal cycle from 1966 to 1980 is consistent with a seasonal variation in the transfer of "bomb" $^{14}CO_2$ from the stratosphere to the troposphere. The decay in the amplitude of this cycle is then explained by the depletion of the stratospheric inventory. Because mixing within the Southern Hemisphere troposphere occurs within a few months, we assume that the amplitude of the seasonal component seen at the surface is proportional to the amount of $^{14}CO_2$ transferred from stratosphere to troposphere in the previous few months. If this is assumed to be proportional to the $^{14}CO_2$ inventory in the stratosphere, modulated by the seasonally varying exchange rate, then the 12-yr decay time of the seasonal cycle is equal to the mean residence time for stratospheric CO_2.

This estimate of stratospheric mean residence time is longer than the value of 7.0 yr (half-life of 58 months) derived by Telegadas (1971) from measurements of ^{14}C in the stratosphere up to 1969. This earlier data may reflect a residence time for just the lower part of the stratosphere. The value derived here is closer to an alternative estimate of 10 yr for the mean residence time of air in the stratosphere based on energy and mass flux (Walker 1977).

COMPARISON OF $^{14}CO_2$ DATA WITH ATMOSPHERIC TRANSPORT MODELS

Modeling of tracer transport in the atmosphere due to advection and diffusion has progressed considerably in recent years (Mahlman, Levy & Moxim 1980; Golombek & Prinn 1986). Models that incorporate consistent global circulation and realistic (if approximate) climatology can now be used to predict tracer concentrations. This approach is preferable to inferring atmospheric transport from tracer data alone.

We now present some results using a two-dimensional model for atmospheric transport (Plumb & Mahlman 1987; Plumb & McConalogue 1988) which is a zonally averaged version of a larger three-dimensional global circulation model (GCM) (Mahlman & Moxim 1978). The zonally averaged version gives the same net tracer transport as the three-dimensional model, but requires much less computer time. A resolution of 2.4° in latitude and 10 vertical levels extending to the 10mBar level (33km) are used.

The vertical diffusion coefficients at the lowest two layers were increased to $8m^2s^{-1}$ (bottom level) and $6m^2s^{-1}$ (next lowest level), based on other work using this model for determining seasonal variation of atmospheric CO_2 concentrations (Plumb, pers commun). Otherwise the fields determining atmospheric transport are as determined from the three-dimensional GCM.

To relate our South Pacific $^{14}CO_2$ data with this model, it was run from an initial condition where a tracer is injected instantaneously with uniform concentration throughout the lower three grid layers of the stratosphere representing pressure levels 110, 65 and 38mbar. The only sink for the tracer is at the surface, where there is a uniform sink strength set to give approximately the observed overall decay rate from 1966 onwards. Figure 5 shows the tracer concentration at 45°S predicted by the model. Note that results for the first two years are sensitive to the artificial initial conditions. Figure 6 shows a month plot, in the same format as Figure 4A, of the seasonal component of this predicted time series, extracted using the STL procedure after removal of the first two years of data.

There is a significant discrepancy in phase between the predicted seasonal cycle in Figure 6 and the observed one in Figure 4A. The model predicts that the concentration of a tracer injected into the stratosphere will peak in September and reach a minimum in January, almost totally out of phase with the observed result. This implies that either the seasonality of vertical transport in the model is incorrect or the observed seasonal cycle in $^{14}CO_2$ is determined by effects other than seasonality in transport from the stratosphere.

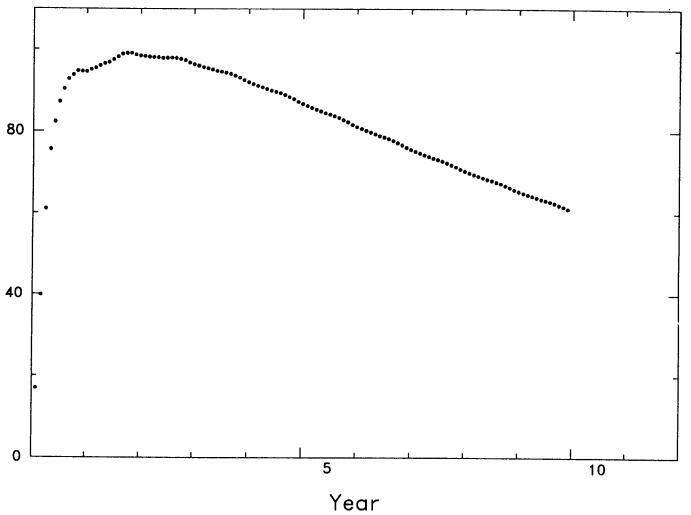

Fig 5. Predicted concentration of tracer at 45°S after a stratospheric injection in the two-dimensional model discussed in the text. The units on the vertical axis are arbitrary.

The seasonal cycles for ^{90}Sr and ^{3}H in the Southern Hemisphere (Taylor 1968) are different from that given here for $^{14}CO_2$. As already mentioned, different transport effects determine the concentration of these isotopes observed at the surface. ^{90}Sr is deposited by aerosols with tropospheric lifetimes on the order of weeks, so its annual cycle at the surface closely follows variations in input from the stratosphere. In contrast, variations in the long-lived $^{14}CO_2$ should lag behind, and in fact be almost completely out of phase with their input from the stratosphere. Comparing Taylor's results with ours shows the $^{14}CO_2$ cycle lags by ca 5 months, much as expected. As the ^{90}Sr and $^{14}CO_2$ data support one another, we believe that the annual cycle in transport between the stratosphere and the troposphere as used in the zonally averaged GFDL model is incorrect.

$^{14}CH_4$ MEASUREMENTS IN THE SOUTH PACIFIC

There are many known sources of atmospheric methane (Khalil & Rasmussen 1983). The major sources appear to be biogenic, such as ruminant animals and rice paddies, in which methane is produced by anaerobic bacteria. Further, atmospheric methane concentra-

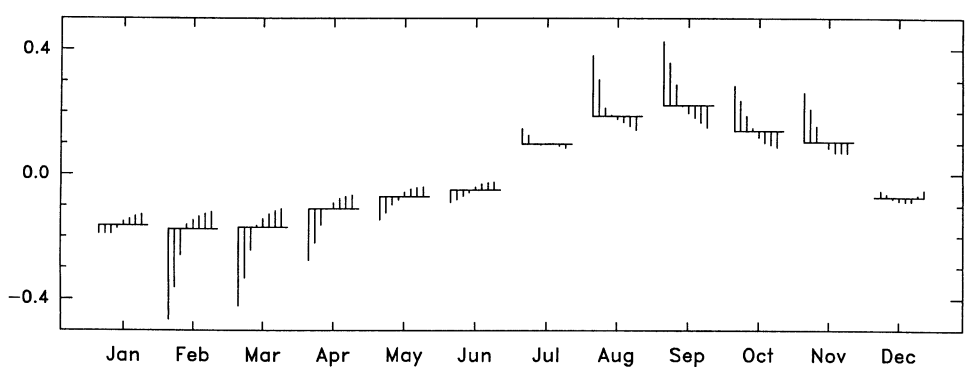

Fig 6. The seasonal cycle in the predicted concentration of tracer at 45°S after a stratospheric injection in the two-dimensional model discussed in the text. The format is as used in Figure 4 and the units on the vertical axis are arbitrary.

https://doi.org/10.1017/S0033822200039941 Published online by Cambridge University Press

tions have been increasing at ca 1%/a over recent decades, suggesting an increasing source strength.

Measurement of ^{14}C in atmospheric methane provides a way to determine the relative amount of methane released from fossil fuel and primordial methane sources (Ehhalt 1973). Lowe *et al* (1988) recently reported Accelerator Mass Spectrometry (AMS) measurements from the South Pacific which showed lower ($^{14}C/^{12}C$) ratios than anticipated, and indicated a significant (25–35%) component of recently released methane has been of fossil origin. Carbon isotope measurements of atmospheric methane from clean air, extending those given by Lowe *et al* and using the same sampling techniques, are shown in Table 3. We include 7 new measurements and omit 2 reported earlier which do not meet stricter consistency criteria now imposed on our AMS data to screen out unsatisfactory graphite targets.

All reported methane samples were taken at Baring Head (41°S, 175°E) near Wellington, New Zealand, under baseline conditions, *ie*, periods of strong onshore winds and while simultaneously measured CO_2 concentrations indicate well-mixed air. The sample mean and standard deviation for $\delta^{14}C$ values in Table 3 is $+78 \pm 94‰$. The sample standard deviation is higher than the mean error associated with the AMS measurement, and this indicates some noise due to sampling and CH_4 extraction procedures.

An improved atmospheric methane sampling method is being developed in which sampled air is pumped through a molecular sieve into 67L stainless steel tanks to a pressure of ca 120 psi. Methane is subsequently extracted in the laboratory by oxidation to, and collection of CO_2, after use of a high-efficiency cryogenic trap to remove any residual CO_2 and water vapor in the tanks.

In the next two sections, we indicate the nature of the constraints placed on methane sources by the isotope ratios of atmospheric methane. The analysis is based on a very simple model of methane sources, which classifies these as either "modern" or "fossil" and uses average values for the isotope ratios of each. Allowance is also made for $^{14}CH_4$ from nuclear power plants. A more realistic model would incorporate sources of intermediate age, such as

TABLE 3
Carbon isotopic composition of atmospheric methane collected at Baring Head, New Zealand, under baseline conditions

Date coll	$\delta^{13}C$ (‰)	pMC % mod	$\delta^{14}C$ (‰)	Lab no.
870312	-47.24 ± 0.05	102.7 ± 5.4	-19 ± 52	NZA-47
870316	-47.03 ± 0.05	106.8 ± 3.3	+20 ± 32	NZA-62
870317	-48.90 ± 0.05	102.3 ± 5.7	-27 ± 54	NZA 46
870410	-46.10 ± 0.05	106.7 ± 2.6	+21 ± 25	NZA 52
870616	-45.68 ± 0.05	105.4 ± 5.2	+10 ± 50	NZA105
870619	-45.57 ± 0.05	104.0 ± 4.5	-3 ± 43	NZA117
870626	-45.96 ± 0.05	109.5 ± 3.6	+48 ± 34	NZA119
870626	-48.59 ± 0.05	129.1 ± 6.5	+229 ± 62	NZA135
870626	-46.37 ± 0.05	111.2 ± 5.8	+64 ± 55	NZA142
870702	-45.80 ± 0.05	131.3 ± 5.4	+258 ± 52	NZA143
870715	-42.57 ± 0.05	122.4 ± 4.7	+180 ± 45	NZA201
870723	-46.62 ± 0.05	105.8 ± 10.0	+12 ± 96	NZA128
870812	-45.05 ± 0.05	118.7 ± 7.9	+138 ± 76	NZA150
870923	-40.	122.7 ± 4.4	+189 ± 42	NZA225
871117	-46.9 ± 0.05	115.9 ± 4.8	+107 ± 46	NZA226
880317	-45.9 ± 0.05	119.7 ± 9.0	+146 ± 87	NZA273
880412	-43.9 ± 0.05	97.8 ± 2.7	-60 ± 26	NZA297
880513	-43.79 ± 0.05	113.6 ± 4.8	+93 ± 46	NZA305

swamps, and use direct isotope measurements of a range of sources with appropriate source strengths. However, the simpler analysis gives an upper estimate for the proportion of methane derived from fossil fuel, and demonstrates the sensitivity of such estimates to some general parameters of atmospheric transport and chemistry.

A TWO BOX ATMOSPHERE MODEL FOR CH_4 ISOTOPES

To interpret the $^{14}CH_4$ data above, we use a model treating the two hemispheres as well-mixed boxes with mass balanced exchange and consider the inventories of CH_4, $^{13}CH_4$ and $^{14}CH_4$ separately. The changes in inventories are related to fluxes by

$$\frac{d}{dt} C_h = Q_h - k\,(C_h - C_{h'}) - \lambda C_h$$

$$\frac{d}{dt} {}^{13}C_h = {}^{13}Q_h - k\,({}^{13}C_h - {}^{13}C_{h'}) - \epsilon\lambda\, {}^{13}C_h$$

$$\frac{d}{dt} {}^{14}C_h = {}^{14}Q_h - k\,({}^{14}C_h - {}^{14}C_{h'}) - \epsilon^2\lambda\, {}^{14}C_h \qquad (1)$$

where:

h	labels the hemisphere S or N;
h'	labels the alternate hemisphere;
C_h, $^{13}C_h$ and $^{14}C_h$	are the inventories of CH_4, $^{13}CH_4$ and $^{14}CH_4$ in hemisphere h;
Q_h, $^{13}Q_h$ and $^{14}Q_h$	are the source fluxes of CH_4, $^{13}CH_4$ and $^{14}CH_4$ into hemisphere h;
k	is the inter-hemispheric fractional exchange coefficient, taken to be (2 yr)$^{-1}$;
λ	is the inverse mean life of CH_4, taken to be (9.6 yr)$^{-1}$ following Prinn *et al* (1987). Note that the small difference between the mean life of $^{12}CH_4$ and CH_4 is ignored here;
ϵ	is the kinetic isotope effect coefficient, taken to be 0.990 ± 0.007 following Davidson *et al* (1987) ((k_{13}/k_{12}) in their notation).

The solution of these equations can be written as

$$C_N(t) + C_S(t) = \int_{-\infty}^{t} e^{\lambda(x-t)}\,(Q_N(x) + Q_S(x))\,dx$$

$$C_N(t) - C_S(t) = \int_{-\infty}^{t} e^{(2k+\lambda)(x-t)}\,(Q_N(x) - Q_S(x))\,dx \qquad (2)$$

with similar equations for ^{13}C and ^{14}C.

The inventories are sensitive to the source flux terms Q only over the last few mean lifetimes of CH_4, *ie*, over the last few decades. For the recent past, we assume that the total CH_4 source flux has increased exponentially at 1%/a and further that the regional distribution of fluxes has remained constant. Then

$$Q_N(x) + Q_S(x) = Q_{\text{tot}}\, e^{\mu(x-1987)}$$

$$Q_N(x) - Q_S(x) = \Delta Q_{\text{tot}}\, e^{\mu(x-1987)} \qquad (3)$$

where:

Q_{tot}	is the total CH_4 release/a in 1987;
ΔQ_{tot}	is the excess release in the Northern Hemisphere over the Southern Hemisphere;
μ	is the exponential increase rate, taken as 0.01.

https://doi.org/10.1017/S0033822200039941 Published online by Cambridge University Press

Evaluating the appropriate integrals in equation (2) we have for the total CH_4 inventories:

$$C_N(t) + C_S(t) = \frac{Q_{\text{tot}}}{\lambda + \mu} e^{\mu(t-1987)}$$

$$C_N(t) - C_S(t) = \frac{\Delta Q_{\text{tot}}}{2k + \lambda + \mu} e^{\mu(t-1987)}. \quad (4)$$

Assuming, in 1987, a mean atmospheric CH_4 concentration of 1670 ppb, and an interhemispheric difference of 90 ppb (Steele *et al* 1987; Fraser *et al* 1986), an atmospheric mass of 1.82×10^{20} moles, and values of λ, μ and k already quoted, we have

$$Q_{\text{tot}} = 3.47 \times 10^{13} \text{ moles/a}$$

$$\Delta Q_{\text{tot}} = 0.91 \times 10^{13} \text{ moles/a}.$$

To determine the inventories of $^{13}CH_4$ and $^{14}CH_4$, we assume that the CH_4 source can be separated into fossil and modern carbon components each having different isotope ratios, which together with the relative proportions of the two sources, have not changed in recent decades. Then

$$^{13}Q_h(t) = (1 + \alpha\, ^{13}\delta_{\text{fos}} + (1 - \alpha)\, ^{13}\delta_{\text{mod}})\, ^{13}R_0 Q_h(t) \quad (5)$$

where:

α is the fossil carbon fraction of the total CH_4 source
$^{13}R_0$ is the ($^{13}C/^{12}C$) ratio of the PDB standard
$^{13}\delta_{\text{fos}}$ is the $\delta^{13}C_{\text{PDB}}$ of the fossil carbon CH_4 source
$^{13}\delta_{\text{mod}}$ is the $\delta^{13}C_{\text{PDB}}$ of the modern carbon CH_4 source.

The inventories resulting from these fluxes are given by

$$^{13}C_N(t) + {}^{13}C_S(t) = (1 + \alpha\, ^{13}\delta_{\text{fos}} + (1 - \alpha)^{13}\delta_{\text{mod}})\, ^{13}R_0 \frac{Q_{\text{tot}}}{\epsilon\lambda + \mu} e^{\mu(t-1987)}$$

$$^{13}C_N(t) - {}^{13}C_S(t) = (1 + \alpha^{13}\delta_{\text{fos}} + (1 - \alpha)\, ^{13}\delta_{\text{mod}})\, ^{13}R_0 \frac{\Delta Q_{\text{tot}}}{2k + \epsilon\lambda + \mu} e^{\mu(t-1987)}. \quad (6)$$

Turning next to $^{14}CH_4$, note that the fossil carbon source has no contribution to Q_h, but that a nuclear power source (Povinec, Chudy & Sivo 1986) must be considered even though this is a negligible source of total CH_4. Thus

$$^{14}Q_N(t) = (1 - \alpha)\,(1 + {}^{14}\delta_{\text{mod}}(t))\, ^{14}R_0 Q_N(t) + {}^{14}Q_{\text{Nuc}}(t)$$

$$^{14}Q_S(t) = (1 - \alpha)\,(1 + {}^{14}\delta_{\text{mod}}(t))^{14}R_0 Q_S(t) \quad (7)$$

where:

$^{14}\delta_{\text{mod}}(t)$ is the mean $\delta^{14}C$ of the modern carbon source
$^{14}R_0$ is the ($^{14}C/^{12}C$) ratio of the modern ^{14}C standard (0.95 NBS oxalic acid), taken to be 1.176×10^{-12} following Karleen *et al* (1964) and
$^{14}Q_{\text{Nuc}}(t)$ is the nuclear power source term.

https://doi.org/10.1017/S0033822200039941 Published online by Cambridge University Press

This leads to

$$^{14}C_N(t) + {}^{14}C_S(t) = \int_{-\infty}^{t} e^{\epsilon^2\lambda(x-t)} \left[(1-\alpha)\,(1 + {}^{14}\delta_{\text{mod}})\,{}^{14}R_0\,Q_{\text{tot}}\,e^{\mu(x-1987)} + {}^{14}Q_{\text{Nuc}}(x)\right] dx$$

$$^{14}C_N(t) - {}^{14}C_s(t) = \int_{-\infty}^{t} e^{(2k+\epsilon^2\lambda)(x-t)} \left[(1-\alpha)\right.$$

$$\left. \cdot\,(1 + {}^{14}\delta_{\text{mod}})\,{}^{14}R^0\,\Delta Q_{\text{tot}}\,e^{\mu(x-1987)} + {}^{14}Q_{\text{Nuc}}(x)\right] dx. \quad (8)$$

The value of $^{14}\delta_{\text{mod}}(t)$ has changed with time due to changes in the $\delta^{14}C$ of atmospheric CO_2 which provides the carbon from which the modern CH_4 is derived. We assume a residence time of one year between carbon photosynthesis and methane production, and correct for fractionation to $\delta^{13}C$ of $-65‰$ (note this is the inferred value of $\delta^{13}C$ for the modern carbon CH_4 source—see below). Thus

$$(1 + {}^{14}\delta_{\text{mod}}(t)) = \left(\frac{1 - 65‰}{1 - 25‰}\right)^2 (1 + \Delta^{14}C_{\text{atm}}(t-1)) \quad (9)$$

where $\Delta^{14}C_{\text{atm}}(t)$ is the atmospheric $\Delta^{14}C$ value for time t. In order to estimate this last term, we use an average of the atmospheric ^{14}C data of Levin *et al* (1985) representing the Northern Hemisphere, and the atmospheric ^{14}C data given here representing the Southern Hemisphere. Where the Northern Hemisphere data is missing we assume it is the same as the Southern Hemisphere, and prior to 1955 we assume a constant value of $-20‰$. The lower limit of the integration range in equation (8) is taken as 1940, as the integrands become negligible prior to this. Numerical integration then produces

$$\int_{-\infty}^{1987} (1 + {}^{14}\delta_{\text{mod}})\,e^{(\epsilon^2\lambda+\mu)(x-1987)}\,dx = 10.718$$

$$\int_{-\infty}^{1987} (1 + {}^{14}\delta_{\text{mod}})\,e^{(2k+\epsilon^2\lambda+\mu)(x-1987)}\,dx = 1.0037. \quad (10)$$

Levin (pers commun) has estimated the nuclear power term $Q_{Nuc}(t)$ and we use her estimates here. In 1987 the estimated release rate is 1100 Ci/a, corresponding to 17.6 moles of $^{14}CH_4$/a. This is more conveniently expressed as $0.43\ {}^{14}R_0Q_{\text{tot}}$, based on the value of Q_{tot} given above. Using Levin's exponential growth rates, we have

$$Q_{\text{Nuc}}(t) = 0.43\ {}^{14}R_0Q_{\text{tot}}\,e^{0.16(t-1987)}, \text{ for } t = 1975 \text{ to } 1987,$$

$$Q_{\text{Nuc}}(t) = 0.063\ {}^{14}R_0Q_{\text{tot}}\,e^{0.26(t-1975)}, \text{ for } t = 1969 \text{ to } 1975 \text{ and}$$

$$Q_{\text{Nuc}}(t) = 0, \text{ for } t \le 1969. \quad (11)$$

The integrals in equation (8) involving Q_{Nuc} can now be evaluated as

$$\int_{-\infty}^{1987} e^{\epsilon^2\lambda(x-1987)}\,Q_{\text{Nuc}}(x)\,dx = 1.6153\ {}^{14}R_0Q_{\text{tot}}$$

$$\int_{-\infty}^{1987} e^{(2k+\epsilon^2\lambda)(x-1987)}\,Q_{\text{Nuc}}(x)\,dx = 0.3407\ {}^{14}R_0Q_{\text{tot}}. \quad (12)$$

INTERPRETATION OF $^{14}CH_4$ DATA

We can now calculate α, the fossil carbon fraction, from observed $\delta^{14}C$ values for atmospheric CH_4. To summarize, values of k, λ, μ, and mean hemispheric CH_4 concentrations are used to estimate Q_{tot} and ΔQ_{tot}; then estimates of ϵ, $^{14}\delta_{\text{mod}}(t)$ and $^{14}Q_{\text{Nuc}}(t)$ are used to calculate the hemispheric $^{14}CH_4$ inventories relative to the total CH_4 inventory in terms of

https://doi.org/10.1017/S0033822200039941 Published online by Cambridge University Press

an unknown α. Finally, we relate the inventory ratio to the observed $\delta^{14}C$ using

$$\frac{^{14}C_S}{C_S} = {}^{14}R_0\,(1 + \delta^{14}C_{obs}) \tag{13}$$

giving an equation which is solved for α. With the parameters values given above, this leads to

$$1.226\,(1 - \alpha) + 0.150 = (1 + \delta^{14}C_{obs})$$

where 1.226 is the value of $(1 + \delta^{14}C)$ that would arise if the only source was from modern carbon, and 0.150 is the shift due to the nuclear power source. From these values we have $\alpha = 0.243$.

Consistency of the $^{13}CH_4$ and $^{14}CH_4$ budgets is now considered. Equation 6 predicts a slight difference in the $\delta^{13}C$ values of CH_4 for the two hemispheres. This arises because the larger source term in the Northern Hemisphere leads to a net export of aged (and, due to the kinetic oxidation effect, heavier) CH_4 to the Southern Hemisphere. Ignoring this very small effect, we have

$$1 + \delta^{13}C_{obs} \approx \frac{\lambda + \mu}{\epsilon\lambda + \mu}\,(1 + \alpha\,{}^{13}\delta_{fos} + (1 - \alpha)\,{}^{13}\delta_{mod})$$

or, to a good approximation

$$\delta^{13}C_{obs} \approx \alpha\,{}^{13}\delta_{fos} + (1 - \alpha)\,{}^{13}\delta_{mod} + 9‰. \tag{14}$$

If the fossil CH_4 source is assumed to be entirely from fossil fuels then the value of $^{13}\delta_{fos}$ should be ca $-30‰$ and, in order to explain $\delta^{13}C_{obs} = -47‰$, we must have $^{13}\delta_{mod} \approx -65‰$. Although this inferred value is slightly lighter than that used in other CH_4 budgets (eg, Tyler, Blake & Rowland 1987; Stevens & Engelkemeir 1988), it is well within the range of $\delta^{13}C$ values of the known sources of modern carbon CH_4. Equation 13, based on observed ^{14}C values, gives a more reliable estimate of α than Equation 14, based on ^{13}C values, because of the considerable uncertainty in $^{13}\delta_{mod}$ in the latter. Thus, we have used equation 13 to determine α and equation 14 to check consistency.

To estimate the sensitivity of α to the parameters of this two-box model, we consider the effect of making variations in these parameters of the order of their uncertainties. This leads to

parameters as described above	$\alpha = 0.243$
k changed from $(2\ yr)^{-1}$ to $(1\ yr)^{-1}$	$\alpha = 0.255$
λ changed from $(9.6\ yr)^{-1}$ to $(8.6\ yr)^{-1}$	$\alpha = 0.252$
ϵ changed from 0.990 to 0.997	$\alpha = 0.233$
Q_{Nuc} reduced to half equation (11)	$\alpha = 0.182$
$\delta^{14}C_{obs}$ changed from $+78‰$ to $+172‰$	$\alpha = 0.166$.

This shows that α is not very sensitive to the methane lifetime estimate, the kinetic isotope effect or the inter-hemispheric exchange time. Yet it is sensitive to the magnitude of the nuclear power source term, and to the value of $^{14}\delta_{obs}$. The estimated growth rate of 17%/a in the total nuclear power $^{14}CH_4$ should cause a significant increase in the $\delta^{14}C$ of atmospheric CH_4. The figures used in the previous section imply an increase in the Southern Hemisphere of ca $25‰$/a and, provided the fossil carbon fraction α is not also increasing, this should be clearly measurable after 2 to 3 years of measurements.

A more detailed calculation of the transport of methane between the hemispheres has been carried out using the zonally averaged atmospheric transport model already described.

https://doi.org/10.1017/S0033822200039941 Published online by Cambridge University Press

When the model is run with a northern mid-latitude tracer source and a uniformly distributed sink corresponding to a tracer lifetime of 10 yr, the difference between the predicted values of the tracer concentrations at 45°N and 45°S corresponds to a 2.5-yr inter-hemispheric exchange time. This supports the value of k used above.

CONCLUSION

Our 32-yr record of atmospheric $^{14}CO_2$ measurements in the South Pacific covers nearly all the period in which atmospheric ^{14}C has been influenced by nuclear weapons testing, and begins with $\Delta^{14}C$ values below zero. Since 1966 the decrease of this "bomb" carbon in the atmosphere has roughly followed an exponential decay with a 1/e time of 17 yr. From 1966–1977, the $^{14}CO_2$ data show a small latitudinal variation, and a definite seasonal cycle peaking in February. This seasonal cycle in $^{14}CO_2$ is believed due to seasonal changes in the rate of transport of "bomb" carbon from the stratosphere and is consistent with the cycle of other fallout products. The cycle decayed in amplitude with a 1/e time of 12 yr, which is inferred to be the mean residence time for CO_2 in the stratosphere.

A two-dimensional model of atmospheric transport based on a three dimensional general circulation model predicts a seasonal cycle in the arrival of a tracer injected into the stratosphere, but the phase of the predicted cycle disagrees with that observed for $^{14}CO_2$. It would seem that stratosphere-to-troposphere transport is not estimated correctly in the model.

An analysis of $^{14}CH_4$ data has shown how these can be used to estimate the fraction of atmospheric methane derived from fossil carbon. A major uncertainty in this estimate appears to be the contribution of nuclear power plants to $^{14}CH_4$ in the atmosphere. However, comparable measurements in both hemispheres over a number of years should enable the nuclear power source of CH_4 to be better determined.

ACKNOWLEDGMENTS

The atmospheric $^{14}CO_2$ data presented here are the result of the work of many people. We wish to acknowledge the contribution of M K Burr, who was responsible for maintaining our gas counters for much of the period covered. Sampling at the Wellington site was done by the staff of the New Zealand Post Office Makara radio station; at the South Pacific island sites, by meteorological observers from the New Zealand Meteorological Service; at Scott Base, by staff of the Antarctic division, DSIR, and at Melbourne, by E D Gill of the National Museum of Victoria. We are grateful for the assistance of all these people.

R A Plumb kindly provided the source code and transport coefficients for the zonally averaged model of atmospheric transport, and his support and guidance in the use of this model are much appreciated. We would also like to thank W S Cleveland for supplying code for his STL procedure. Finally, we would like to pay tribute to T A Rafter, who had the foresight to begin measurements of atmospheric $^{14}CO_2$ in New Zealand, and who recognized the importance of extending these to other South Pacific sites many years ago.

References

Cleveland, W S 1979 Robust locally weighted regression and smoothing scatterplots. *Jour Am Statistical Assoc* 74: 829–836.

Cleveland, W S, Freeny, E and Graedel, T E 1983 The seasonal component of atmospheric CO_2: Information from new approaches to the decomposition of seasonal time series. *Jour Geophys Research* 88: 10934–10946.

Cleveland, W S and McRae, J E 1989 The use of loess and STL in the analysis of atmospheric CO_2 and related data. *In* Elliott, W P, ed, The statistical treatment of CO_2 data records. *NOAA Tech Memo* ERL ARL-173, Silver Spring, Maryland.

Davidson, J A, Cantrell, C A, Tyler, S C, Shetter, R E, Cicerone, R J and Calvert, J G 1987 Carbon kinetic isotope effect in the reaction of CH_4 with HO. *Jour Geophys Research* 92: 2195–2199.

Ehhalt, D H 1973 Methane in the atmosphere. *In* Carbon and the biosphere. *Brookhaven symposium in biology,* 24th, Proc. Upton, New York, USAEC, CONF-720510.

Enting, I G 1987 On the use of smoothing splines to filter CO_2 data. *Jour Geophys Research* 92: 10977–10984.

Enting, I G and Pearman, G I 1983 Refinements to a one-dimensional carbon cycle model. *CSIRO Div Atmos Research tech paper* 3.

Fraser, P J, Hyson, P, Rasmussen, R A, Crawford, A J and Khalil, M A K 1986 Methane, carbon monoxide and methylchloroform in the Southern Hemisphere. *Jour Atmos Chem* 4: 3–42.

Golombek, A and Prinn, R G 1986 A global three-dimensional model of the circulation and chemistry of $CFCl_3$, CF_2Cl_2, CH_3CCl_3, CCl_4, and N_2O. *Jour Geophys Research* 91: 3985–4001.
Heimann, M and Keeling, C D 1986 Meridional eddy diffusion model of the transport of atmospheric carbon dioxide, 1. Seasonal carbon cycle over the tropical Pacific ocean. *Jour Geophys Research* 91: 7765–7781.
Karlen, I, Olsson, I, U, Kallberg, P and Kilicci, S 1964 Absolute determination of the activity of two ^{14}C dating standards. *Arkiv Geofysik* 4: 465–471.
Keeling, C D, Mook, W G and Tans, P P 1979 Recent trends in the $^{13}C/^{12}C$ ratio of atmospheric carbon dioxide. *Nature* 277: 121–123.
Khalil, M A K and Rasmussen, R A 1983 Sources, sinks and seasonal cycles of atmospheric methane. *Jour Geophys Research* 88: 5131–5144.
Lal, D and Peters, B 1962 Cosmic ray produced isotopes and their application to problems in geophysics. *Progress in elementary particle and cosmic ray physics.* Amsterdam, North Holland 6: 1–74.
Levin, I (ms) 1985 Atmospheric CO_2 in continental Europe—An alternative approach to clean air CO_2 data. Paper presented at IAMAP mtg, Atmospheric carbon dioxide its sources, sinks, and global transport, Kandersteg, Switzerland.
Levin, I, Kromer, B, Schoch-Fischer, H, Bruns, M, Münnich, M, Berdau, D, Vogel, J C and Münnich, K O 1985, 25 years of tropospheric ^{14}C observations in central Europe. *Radiocarbon* 27(1): 1–19.
Logan, J A, Prather, M J, Wofsy, S C and McElroy, M B 1981 Tropospheric chemistry: A global perspective. *Jour Geophys Research* 86: 7210–7254.
Lowe, D C, Brenninkmeijer, C A M, Manning, M R, Sparks, R and Wallace, G 1988 Radiocarbon determination of atmospheric methane at Baring Head, New Zealand. *Nature* 332: 522–525.
Mahlman, J D, Levy, H and Moxim, W J 1980 Three dimensional tracer structure and behaviour as simulated in two ozone precursor experiments. *Jour Atmos Sci* 37: 655–685.
Mahlman, J D and Moxim, W J 1978 Tracer simulation using a global general circulation model: results from a midlatitude instantaneous source experiment. *Jour Atmos Sci* 35:1340–1374.
Nydal, R and Lovseth, K 1983 Tracing bomb ^{14}C in the atmosphere 1962—1980. *Jour Geophys Research* 88: 3621–3642.
Oeschger, H, Siegenthaler, U, Schotterer, U and Gugelmann, A 1975 A box diffusion model to study the carbon dioxide exchange in nature. *Tellus* 27: 168–192.
Peng, T-H, Broecker, W S, Freyer, H D and Trumbore, S 1983 A deconvolution of the tree ring based $\delta^{13}C$ record. *Jour Geophys Research* 88: 3609–3620.
Plumb, R A and Mahlman, J D 1987 The zonally averaged transport characteristics of the GFDL general circulation /transport model. *Jour Atmos Sci* 4:298–326.
Plumb, R A and McConalogue, D D 1988 On the meridional structure of long-lived tropospheric constituents. *Jour Geophys Research* 93: 15,897–15,913.
Povinec, P, Chudy, M and Sivo, A 1986 Anthropogenic radiocarbon: past present and future. *In* Stuiver, M and Kra, R S, eds, Internatl ^{14}C conf, 12th, Proc. *Radiocarbon* 28(2A): 668–672.
Prinn, R, Cunnold, D, Rasmussen, R, Simmonds, P, Alyea, F, Crawford, A Fraser, P and Rosen, R 1987 Atmospheric trends in methylchloroform and the global average for the hydroxyl radical. *Science* 238: 945–950.
Rafter, T A 1955 ^{14}C variations in nature and the effect on radiocarbon dating. *New Zealand Jour Sci Tech* 37: 20–38.
Rafter, T A and Fergusson, G J 1959 Atmospheric radiocarbon as a tracer in geophysical circulation problems. *In United Nations peaceful uses of atomic energy,* Internatl conf, 2nd, Proc. London, Pergamon Press.
Rafter, T A and O'Brien, B J 1970 Exchange rates between the atmosphere and the ocean as shown by recent C14 measurements in the south Pacific. *In* Olsson, I U, ed, *Radiocarbon variations and absolute chronology,* Nobel symposium, 12th, Proc. Stockholm, Almqvist & Wiksell.
Reinsch, C M 1967 Smoothing by spline functions. *Num Math* 10: 177–183.
Sarmiento, J L and Gwinn, E 1986 Strontium 90 fallout prediction. *Jour Geophys Research* 91: 7631–7646.
Schell, W R, Sauzay, G and Payne, B R 1974 World distribution of environmental tritium. *In Physical behaviour of radioactive contaminants in the atmosphere,* IAEA and WMO symposium, Proc. Vienna, IAEA-STI/PUB/354, IAEA.
Steele, L P, Fraser, P J, Rasmussen, R A, Khalil, M A K, Conway, T J, Crawford, A J, Gammon, R H, Masarie, K A and Thoning, K W 1987 The global distribution of methane in the troposphere. *Jour Atmos Chem* 5: 125–171.
Stevens, C M and Engelkemeir, A 1988 Stable carbon isotopic composition of methane from some natural and anthropogenic sources. *Jour Geophys Research* 93: 725–733.
Stevens, C M, Krout, L, Walling, D and Venters, A 1972 The isotopic composition of atmospheric carbon monoxide. *Earth Planetary Sci Letters* 16: 147–165.
Stuiver, M and Polach, H A 1977 Discussion: Reporting of ^{14}C data. *Radiocarbon* 19(3): 355–363.
Taylor, C B 1968 A comparison of tritium and strontium-90 fallout in the southern hemisphere. *Tellus* 20: 559–576.
Telegadas, K 1971 The seasonal atmospheric distribution and inventories of excess carbon-14 from March 1955 to July 1969. *US Atomic Energy Comm rept* HASL-243.
Trabalka, J R, ed 1985 Atmospheric carbon dioxide and the global carbon cycle. *US Dept Energy rept* DOE/ER-0239.
Tyler, S C, Blake, D R and Rowland, F S 1987 $^{13}C/^{12}C$ ratio in methane from the flooded Amazon forest. *Jour Geophys Research* 92: 1044–1048.
Volz, A, Ehhalt, D H and Derwent, R G 1981 Seasonal and latitudinal variation of ^{14}CO and the tropospheric concentration of OH radicals. *Jour Geophys Research* 86: 5163–5171.
Walker, J C G 1977 *Evolution of the atmosphere.* New York, MacMillan.